

Electrostatic Redesign of the [Myoglobin, Cytochrome *b*₅] Interface To Create a Well-Defined Docked Complex with Rapid Interprotein Electron Transfer

Peng Xiong, Judith M. Nocek, Amanda K. K. Griffin, Jingyun Wang, and Brian M. Hoffman*

Northwestern University, Department of Chemistry, 2145 Sheridan Road, Evanston, Illinois 60208

Received March 18, 2009; E-mail: j-nocek@northwestern.edu; bmh@northwestern.edu

Interactions between macromolecules are fundamental to most of biology. The goal of understanding and controlling protein–protein interactions has inspired numerous efforts to modulate the binding within high-affinity complexes of known structure,^{1–6} although most alterations serve to weaken binding. To begin such efforts at the other extreme, with a pair of proteins that bind weakly, and by altering them to create a well-defined, highly functional complex, offers a different level of challenge. We here report dramatic progress in creating such a complex between the weakly interacting physiological electron-transfer (ET) partners, myoglobin (Mb) and cytochrome *b*₅ (cyt *b*₅).

Cyt *b*₅ is the electron-carrier “repair” protein that reduces met-Mb⁷ and met-Hb^{8,9} to their O₂-carrying ferroheme forms. Studies of ET between Mb and cyt *b*₅ revealed that they react on a “Dynamic Docking” (DD) energy landscape (Figure 1),^{10–12} on which binding and reactivity are uncoupled: binding is weak and involves an ensemble of nearly isoenergetic configurations, only a few of which are reactive; those few contribute negligibly to binding. The sharp contrast of such behavior with that for the conventional “simple docking” (SD) energy landscape (Figure 1), on which a complex exhibits a well-defined (set of) reactive binding configuration(s), led us to ask whether it was possible to redesign the surface of Mb so that its reaction with cyt *b*₅ instead would occur on an SD landscape, with binding and reactivity no longer being decoupled.

The low affinity of these partners is the consequence of poor shape complementarity, weak overall electrostatic attractions between the highly charged cyt *b*₅ and the nearly neutral Mb ($q_{b_5} = -5.72$ C; $q_{Mb} \sim -0.29$ C), and the absence of optimally placed complementary charge pairs on the surfaces of the partners. Our initial attempt to enhance their affinity electrostatically¹³ by neutralizing the Mb heme propionates through esterification increased the ET rate by ~ 100 -fold but, surprisingly, did not significantly alter the affinity; this observation in fact led us to formulate the DD paradigm.¹⁰

To identify surface residues of Mb where mutation would best enhance *reactive binding*, we performed Brownian Dynamics (BD) simulations¹⁴ of the docking between cyt *b*₅ and all Mb surface charge reversal mutants (D/E \rightarrow K). To probe net binding we used a center-of-mass (COM) criterion to define a BD trajectory “hit”; to probe reactive binding we defined a hit to have a short distance between one O of a cyt *b*₅ heme carboxylate and one O of a Mb heme carboxylate (O–O criterion).^{15,16} The BD profile for Mb(WT) (Figure 2, top left) shows that cyt *b*₅ “binding hits” (COM criterion) are distributed over the entire Mb surface, with some clustering in patches away from the heme edge, and few “reactive hits” (OO criterion) near the Mb(WT) heme edge (Figure 2, top, right). The 20 most stable binding hits (COM criterion) fall at a Mb surface patch “above and to the left” of the heme edge. Among these, there is no correlation of the cyt *b*₅ orientations (backbone rmsd, 11.2

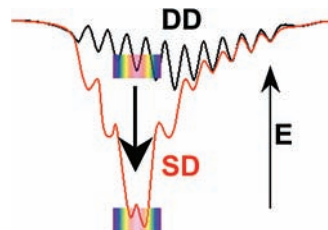


Figure 1. Conversion of “Dynamic Docking” (DD) to “Simple Docking” (SD) energy landscapes; rainbows represent ET-active configurations.

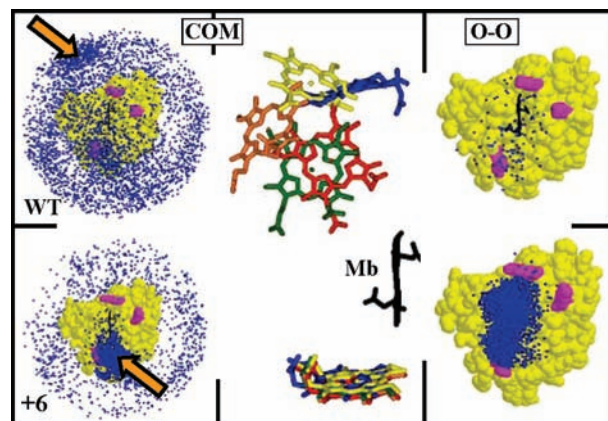


Figure 2. BD simulations for docking Mb(WT) (*upper*) and Mb(+6) (*lower*) to cyt *b*₅ (10⁴ trajectories; pH 7; $\mu = 18$ mM); mutation sites, magenta. “Hit” profiles using COM (Left) and O–O (Right) reaction criteria; blue dots, cyt *b*₅ COM at a hit (see refs 12 and 14). (Center) Mb heme (black) plus superpositions of the cyt *b*₅ hemes for the five most-stable configurations from the COM simulations with Mb(WT) (*upper*), Mb(+6) (*lower*); hemes properly oriented relative to the Mb heme. Arrows on left indicate corresponding locations of the cyt *b*₅ COM relative to Mb face.

\AA)¹⁷ as illustrated by their differing cyt *b*₅ heme orientations (Figure 2, top center).

Not surprisingly, computations with the mutant Mb’s showed that binding of the negatively charged cyt *b*₅ to Mb is opposed by the three acidic residues surrounding the exposed heme on the Mb front face (D44, D60, and E85). We then tested whether the cumulative effects of reversing the charge at these three sites would stabilize the complex in a reactive configuration with the hemes proximate to one another, thereby reshaping the energy landscape to more closely resemble one of simple docking, Figure 1.

Simulations for the triple mutant (Figure 2, lower) indeed show a high density of hits near the Mb heme edge with both criteria. Moreover, the 20 most-stable cyt *b*₅ configurations now correspond to a single well-defined structure (rmsd, 0.6 \AA),¹⁷ as illustrated by the close overlap of their hemes (Figure 2, center, lower) with their heme edges facing that of Mb. Thus, the simulations suggest that cyt *b*₅ might bind strongly to the Mb(+6) triple mutant (D44K/

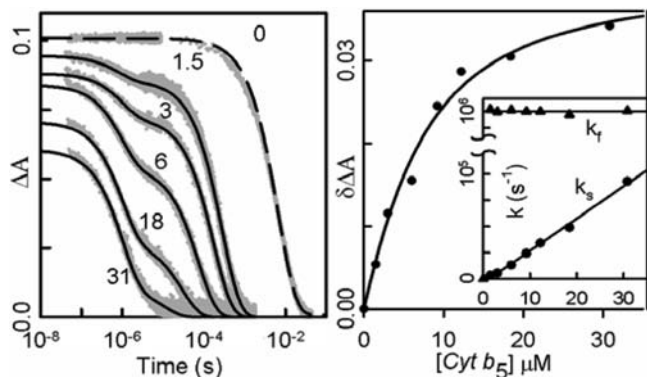


Figure 3. Titration of ZnMb(+6) with $\text{Fe}^{3+}\text{cyt } b_5$. (Left) Triplet decay traces as a function of $[\text{Fe}^{3+}\text{cyt } b_5]$ (μM). Conditions: $5 \mu\text{M}$ ZnMb; 5 mM KPi, pH 6; $20 \text{ }^\circ\text{C}$; 475 nm . (Right) Zero-time absorbance decrease for cyt b_5 binding to Mb(+6) and fit to eq 1: $K_a = 2.2 \times 10^5 \text{ M}^{-1}$; $\delta\Delta A_0^{\text{max}} = 0.042$. (Inset) Rate constants from fitting triplet decays to biexponential.

D60K/E85K) as a reactive “simple-docking” complex in which binding and reactivity are coupled.

To test this possibility, we prepared ZnMb(+6), the (D44K/D60K/E85K) triple mutant substituted with Zn deuteroporphyrin, and monitored binding and ET quenching of the $^3\text{ZnMb}$ triplet state formed by rapid intersystem crossing from the laser-flash generated singlet state of ZnMb.^{18–20}

Throughout a titration of Mb(WT) with $\text{Fe}^{3+}b_5$ at pH 6 ($\mu = 5.3 \text{ mM}$), the ZnMb triplet decay traces remain exponential, with a decay constant (k_{obs}) that increases linearly with $[\text{Fe}^{3+}b_5]$ from the intrinsic decay constant, k_D , without evidence of saturation: $k_{\text{obs}} = k_D + k_2[\text{Fe}^{3+}b_5]$. The slope of this line is the bimolecular quenching rate constant, $k_2 = 4.7 \times 10^6 \text{ M}^{-1} \text{ s}^{-1}$, similar to the value reported previously.^{10,12} The measurements indicate this complex is in fast exchange, $k_{\text{off}} \gg k_{\text{et}}$, where k_{et} represents the apparent intracomplex ET rate constant; as a result, $k_2(\text{WT}) = k_{\text{et}}(\text{WT})K_a(\text{WT})$, where K_a is the overall binding constant. Combination of the measured $k_2(\text{WT})$ and reported value, $K_a(\text{WT}) \approx 10^3 \text{ M}^{-1}$,^{21,22} gives $k_{\text{et}}(\text{WT}) \approx (4\text{--}5) \times 10^3 \text{ s}^{-1}$.

In contrast, the triplet decay traces for ZnMb(+6) are biexponential throughout a titration with $\text{Fe}^{3+}b_5$, and the larger rate constant is invariant with $[\text{Fe}^{3+}b_5]$, $k_f = 10^6 \text{ s}^{-1}$ (Figure 3). These observations indicate that the complex is in slow exchange with its unbound partners ($k_{\text{off}} \ll k_{\text{et}}$) and that the fast phase represents rapid ET quenching within the bound $[\text{ZnMb}, \text{Fe}^{3+}b_5]$ complex: $k_f = k_{\text{et}}(+6) = 10^6 \text{ s}^{-1}$.²³ The rate constant for the slower process increases linearly with addition of $\text{Fe}^{3+}b_5$, $k_s = k_2[\text{Fe}^{3+}b_5] + k_D$, and thus is associated with the bimolecular reaction between free ZnMb(+6) and $\text{Fe}^{3+}b_5$; the second-order rate constant is $k_2 = 3.1 \times 10^9 \text{ M}^{-1} \text{ s}^{-1}$, corresponding to diffusion-limited ET.

Typically, one would fit the cyt b_5 -dependent fraction of the intracomplex phase, $f(\text{Fe}^{3+}b_5)$, with a standard binding isotherm to obtain the binding constant, K_a . However, as seen in Figure 3, the total amplitude of the triplet signal, measured as the extrapolated zero-time amplitude, $\Delta A_0(\text{Fe}^{3+}b_5)$, decreases during a titration, an indication that the bound complex not only exhibits rapid ET from the ZnMb(+6) triplet state to $\text{Fe}^{3+}b_5$ but also extremely rapid intracomplex quenching of the singlet state. We instead determined K_a by obtaining $f(\text{Fe}^{3+}b_5)$ from $\Delta A_0(\text{Fe}^{3+}b_5)$ during a titration by use of the relationship,

$$\begin{aligned} \Delta A_0(0) - \Delta A_0(\text{Fe}^{3+}b_5) &= [\Delta A_0(0) - \Delta A_0(\infty)]f(\text{Fe}^{3+}b_5) \\ \delta\Delta A_0 &= \delta\Delta A_0^{\text{max}}f(\text{Fe}^{3+}b_5) \end{aligned} \quad (1)$$

and fitting $\delta\Delta A_0$ to a binding isotherm. The resulting binding constant, $K_a(+6) = 2.2 \times 10^5 \text{ M}^{-1}$, is more than 2 orders of magnitude greater than that for ZnMb(WT).^{21,22}

Thus, while cyt b_5 reacts with Mb(WT) on a DD energy landscape, with weak binding in multiple configurations—most of which are nonreactive, a low second-order ET rate constant, and rapid exchange ($k_{\text{off}} \gg k_f$) between the complex and its unbound components—it appears that the three charge-reversals around the “front-face” heme edge of Mb(+6) have directed cyt b_5 to a surface area of Mb adjacent to its heme and created a well-defined, most-stable structure (Figure 2) that supports good ET pathways. The mutations indeed appear to have coupled binding and ET, increasing both K_a and k_{et} by a factor of $\sim 2 \times 10^2$, and thus to have induced the sought-for conversion from a DD to an SD energy landscape.

Acknowledgment. We gratefully acknowledge NIH funding for this work (HL063203; GM008382) and Prof. Ishwar Radhakrishnan for assistance with the structural comparisons.

References

- (1) Tetreault, M.; Cusanovich, M.; Meyer, T.; Axelrod, H.; Okamura, M. Y. *Biochemistry* **2002**, *41*, 5807–5815.
- (2) Selzer, T.; Albeck, S.; Schreiber, G. *Nat. Struct. Biol.* **2000**, *7*, 537–541.
- (3) Ivkovic-Jensen, M. M.; Ullmann, G. M.; Young, S.; Hansson, O.; Crnogorac, M. M.; Ejdebaeck, M.; Kostic, N. M. *Biochemistry* **1998**, *37*, 9557–9569.
- (4) Schreiber, G.; Haran, G.; Zhou, H.-X. *Chem. Rev.* **2009**, *109*, 839–860.
- (5) Pearl, N. M.; Jacobson, T.; Meyen, C.; Clementz, A. G.; Ok, E. Y.; Choi, E.; Wilson, K.; Vitello, L. B.; Erman, J. E. *Biochemistry* **2008**, *47*, 2766–2775.
- (6) Davidson, V. L. *Acc. Chem. Res.* **2008**, *41*, 730–738.
- (7) Hagler, L.; Coppes, R. I., Jr.; Herman, R. H. *J. Biol. Chem.* **1979**, *254*, 6505–6514.
- (8) Hultquist, D. E.; Passon, P. G. *Nat. New Biol.* **1971**, *229*, 252–254.
- (9) Kuma, F. *J. Biol. Chem.* **1981**, *256*, 5518–5523.
- (10) Liang, Z.-X.; Nocek, J.; Huang, K.; Hayes, R. T.; Kurnikov, I. V.; Beratan, D. N.; Hoffman, B. M. *J. Am. Chem. Soc.* **2002**, *124*, 6849–6859.
- (11) Liang, Z.-X.; Kurnikov, I. V.; Nocek, J. M.; Mauk, A. G.; Beratan, D. N.; Hoffman, B. M. *J. Am. Chem. Soc.* **2004**, *126*, 2785–2798.
- (12) Wheeler, K. E.; Nocek, J.; Cull, D. A.; Yatsunyk, L. A.; Rosenzweig, A. C.; Hoffman, B. M. *J. Am. Chem. Soc.* **2007**, *129*, 3906–3917.
- (13) Shurki, A.; Strajbl, M.; Schutz, C. N.; Warshel, A. *Methods Enzymol.* **2004**, *380*, 52–84.
- (14) BD computations were done with MacroDox (see: Northrup, S. H.; Thomasson, K. A.; Miller, C. M.; Barker, P. D.; Eltis, L. D.; Guillemette, J. G.; Inglis, S. C.; Mauk, A. G. *Biochemistry* **1993**, *32*, 6613–6623.) using procedures described in ref 12.
- (15) Lin, J.; Balabin, I. A.; Beratan, D. N. *Science* **2005**, *310*, 1311–1313.
- (16) Moser, C. C.; Chobot, S. E.; Page, C. C.; Dutton, P. L. *Biochim. Biophys. Acta* **2008**, *1777*, 1032–1037.
- (17) Configurations were compared using Suppose, available through the Structural Biology Facility at Vanderbilt University.
- (18) Nocek, J. M.; Sishta, B. P.; Cameron, J. C.; Mauk, A. G.; Hoffman, B. M. *J. Am. Chem. Soc.* **1997**, *119*, 2146–2155.
- (19) Trypsin-solubilized bovine cyt b_5 is used.^{10,11} The plasmid for the equine Mb(D44K/D60K) mutant²⁰ was used as a template for Mb(+6), which was overexpressed in *E. coli*, purified, and reconstituted with Zn-deuteroporphyrin IX as in refs 10 and 11; complete characterization will be presented elsewhere. Flash photolysis employed LKS.60 (Applied Photophysics) equipped with a Xe-arc and a frequency-doubled Spectra-Physics INDI 40-10-HG Nd:YAG pulsed laser.
- (20) Hoffman, B. M.; Celis, L. M.; Cull, D. A.; Patel, A. D.; Seifert, J. L.; Wheeler, K. E.; Wang, J.; Yao, J.; Kurnikov, I. V.; Nocek, J. *Proc. Natl. Acad. Sci. U.S.A.* **2005**, *102*, 3564–3569.
- (21) Liang, Z.-X.; Jiang, M.; Ning, Q.; Hoffman, B. M. *JBIC* **2002**, *7*, 580–588.
- (22) Worrall, J. A. R.; Liu, Y.; Crowley, P. B.; Nocek, J.; Hoffman, B. M.; Ubbink, M. *Biochemistry* **2002**, *41*, 11721–11730.
- (23) Preliminary kinetic measurements in viscous solutions suggest that even this ET rate constant involves conformational gating, and not just the ET process itself.

JA902131D